

extreme as some portions of the Martian mantle [e.g., (26)]. Although the Itsaq-DM seems to have been obliterated, or at least not sampled at present, the source mantle of the Narryer Complex crust persists to the present. These observations require an explanation for the differing behavior of the two depleted mantle components, the Narryer-DM able to retain its identity, despite ongoing mantle dynamics for >4.5 Gy, as compared with the transient Itsaq-DM. If all or much of the mantle was initially as highly fractionated as Itsaq-DM, then why was this mantle only partially, but apparently homogeneously, remixed such that all modern terrestrial rocks yield precisely the same ^{142}Nd , distinct from chondrites? The difference supports models of “hidden reservoirs” where part of the complementary, low Sm/Nd domain is locked in a region of Earth, where it is both never sampled at the surface [e.g., (27–29)] and isolated from remixing. More speculative suggestions are that part of the low Sm/Nd component may have been lost from Earth during accretion, with the missing material accounting for the present-day high ^{142}Nd , or that Earth accreted with a nonchondritic Sm/Nd ratio. In contrast, the Itsaq-DM mantle source persisted for at least a billion years after its formation, as recorded by compositions of 3.6-Gy-old Greenland samples, but was able to communicate with other less fractionated mantle reservoirs and eventually lost its distinct signature through remixing.

An enduring tenet of geology is that Earth started from a well-mixed homogeneous body and evolved progressively over geologic time to a more differentiated chemical state through observable processes such as plate tectonics and continental crust formation. The ^{142}Nd data presented here, however, provide strong evidence that terrestrial planets such as Earth were affected by non-uniformitarian processes early in their histories, resulting in locally extreme chemical differentiation. Furthermore, some of the chemical effects of these events appear to persist in silicate domains to the present day. Thus, an emerging challenge for understanding the Earth system is determining the relative roles of early planetary processes versus progressive differentiation in shaping Earth’s chemical architecture.

References and Notes

- L. Nyquist, H. Wiesmann, B. Bansal, *Geochim. Cosmochim. Acta* **59**, 2817 (1995).
- M. Boyet, R. W. Carlson, *Science* **309**, 576 (2005).
- C. N. Foley et al., *Geochim. Cosmochim. Acta* **69**, 4557 (2005).
- K. Rankenburg, A. D. Brandon, C. R. Neal, *Science* **312**, 1369 (2006).
- C. L. Harper, S. B. Jacobsen, *Nature* **360**, 728 (1992).
- M. Boyet et al., *Earth Planet. Sci. Lett.* **214**, 427 (2003).
- G. Caro, B. Bourdon, J.-L. Birck, S. Moorbath, *Nature* **423**, 428 (2003).
- M. Sharma, C. Chen, *Precamb. Res.* **135**, 315 (2004).
- G. Caro, B. Bourdon, J.-L. Birck, S. Moorbath, *Geochim. Cosmochim. Acta* **70**, 164 (2006).
- M. Boyet, R. Carlson, *Earth Planet. Sci. Lett.* **250**, 254 (2006).
- A. Polat, A. W. Hofmann, *Precamb. Res.* **126**, 197 (2003).
- R. Frei, M. Rosing, T. Waight, D. G. Ulbrich, *Geochim. Cosmochim. Acta* **66**, 467 (2002).
- R. Andreasen, M. Sharma, *Science* **314**, 806 (2006).
- R. W. Carlson, M. Boyet, M. Horan, *Science* **316**, 1175 (2007).
- Materials and methods are available as supporting material on Science Online.
- A. Nutman, V. McGregor, C. Friend, V. Bennett, P. Kinny, *Precamb. Res.* **78**, 1 (1996).
- H. Smithies, D. Champion, K. Cassidy, *Precamb. Res.* **127**, 89 (2003).
- A. Nutman, V. Bennett, C. Friend, K. Horie, H. Hidaka, *Contrib. Mineral. Petrol.* **154**, 385 (2007).
- A. Nutman, V. Bennett, P. Kinny, R. Price, *Tectonics* **12**, 97 (1993).
- C. Friend, A. Nutman, *J. Geol. Soc. Lond.* **162**, 147 (2005).
- $\epsilon^{142}\text{Nd}(t) = \left[\frac{^{142}\text{Nd}(t)}{^{144}\text{Nd}(t)} - \frac{^{142}\text{Nd}(t)_{\text{CHUR}}}{^{144}\text{Nd}(t)_{\text{CHUR}}} \right] \times 10^4$, where t refers to the crystallization age of the sample and CHUR is the chondritic reservoir composition used to represent bulk silicate Earth with present-day $^{143}\text{Nd}/^{144}\text{Nd} = 0.512638$ and $^{147}\text{Sm}/^{144}\text{Nd} = 0.1966$.
- S. B. Jacobsen, *Annu. Rev. Earth Planet. Sci.* **33**, 531 (2005).
- W. B. Tonks, H. J. Melosh, *J. Geophys. Res.* **98**, 5319 (1993).
- Y. Abe, *Phys. Earth and Planet. Int.* **100**, 27 (1997).
- M. Boyet, R. Carlson, *Earth Planet. Sci. Lett.* **262**, 505 (2007).
- L. Borg, D. Draper, *Meteoritics Planet. Sci.* **34**, 439 (2003).
- C. Chase, P. J. Patchett, *Earth Planet. Sci. Lett.* **91**, 66 (1988).
- J. Blichert-Toft, F. Albarède, *Earth Planet. Sci. Lett.* **148**, 243 (1997).
- I. Tolstikhin, A. W. Hofmann, *Phys. Earth Planet. Int.* **148**, 109 (2005).
- Y. Amelin et al., *Science* **297**, 1678 (2002).
- Y. Amelin, A. Ghosh, E. Rotenberg, *Geochim. Cosmochim. Acta* **69**, 505 (2005).
- Greenland investigations by V.C.B. and A.P.N. were supported by Australian Research Council Discovery grant DP0342794. The manuscript was improved by the extensive comments of two anonymous reviewers and R. Carlson. V.C.B. thanks M. Norman and G. Caro for helpful discussions at various stages of this project.

Supporting Online Material

www.sciencemag.org/cgi/content/full/318/5858/1907/DC1
Materials and Methods
Figs. S1 to S3
Tables S1 to S3
References

31 May 2007; accepted 30 October 2007
10.1126/science.1145928

High-Pressure Creep of Serpentine, Interseismic Deformation, and Initiation of Subduction

Nadege Hilairt,^{1*} Bruno Reynard,¹ Yanbin Wang,² Isabelle Daniel,¹ Sebastien Merkel,³ Norimasa Nishiyama,²† Sylvain Petitgirard¹

The supposed low viscosity of serpentine may strongly influence subduction-zone dynamics at all time scales, but until now its role could not be quantified because measurements relevant to intermediate-depth settings were lacking. Deformation experiments on the serpentine antigorite at high pressures and temperatures (1 to 4 gigapascals, 200° to 500°C) showed that the viscosity of serpentine is much lower than that of the major mantle-forming minerals. Regardless of the temperature, low-viscosity serpentinized mantle at the slab surface can localize deformation, impede stress buildup, and limit the downdip propagation of large earthquakes at subduction zones. Antigorite enables viscous relaxation with characteristic times comparable to those of long-term postseismic deformations after large earthquakes and slow earthquakes. Antigorite viscosity is sufficiently low to make serpentinized faults in the oceanic lithosphere a site for subduction initiation.

Subduction zones, in which slabs of oceanic lithosphere sink into the mantle, are active zones where frequent large earthquakes cause considerable human and material damage. Such events are triggered by stress buildup or strain localization, the understanding of which relies on identifying the materials involved and their rheology. On top of slabs of many subduction zones, a layer with low seismic velocity and high Poisson ratio (>0.29) is interpreted as extensively serpentinized mantle material (1, 2), and may accommodate most of the deformation at the slab/mantle wedge interface. Serpentinites form by peridotite hydration either during hydrothermal alteration of the oceanic lithosphere before subduction or by percolation of the fluids released by mineral dehydration within the downgoing slab through the overlying mantle

wedge (3). The high-pressure variety of serpentine, antigorite, can remain stable down to ~180 km depth in cold subduction zones (4). Serpentinites are highly deformed as compared to other exhumed materials in paleosubduction zones (5), which points to their crucial mechanical role. The expected low strength or viscosity of serpentinite

¹Laboratoire des Sciences de la Terre, CNRS, Ecole Normale Supérieure de Lyon, Université Claude Bernard Lyon 1, 46 Allée d’Italie, 69364 Lyon Cedex 07, France. ²Center for Advanced Radiation Sources, University of Chicago, 5640 South Ellis Avenue, Chicago, IL 60637, USA. ³Laboratoire de Structure et Propriétés de l’Etat Solide, UMR CNRS 8008, Université des Sciences et Technologies de Lille, 59655 Villeneuve d’Ascq, France.

*To whom correspondence should be addressed. E-mail: nadege.hilairt@ens-lyon.fr

†Present address: Geodynamics Research Center, Ehime University, Japan.

has strong seismic implications because it may govern stress buildup and downdip relaxation over the slab surface, which are critical parameters for earthquake triggering and for the downdip extent of major ruptures (6). So far, only viscous relaxation of the anhydrous mantle has been considered a potential trigger of major earthquakes, such as the Tonankai 1944, Nankaido 1946 (7), and Alaska 1964 events (8). Serpentinites also have global geodynamic importance on the time scale of mantle convection because a serpentinite layer may decouple the mantle wedge from the downgoing slab (9). Its presence therefore is a defining condition of the plate tectonic regime on Earth.

The limitations of apparatus have restricted previous high-temperature deformation experiments on serpentinites to pressures below 0.7 GPa (5, 9–11). Below the antigorite dehydration temperature (600°C), such low confining pressures favor brittle behavior, with deformation being governed by frictional forces, whereas different deformation mechanisms are to be expected at higher pressures (11), as suggested by numerous defects allowing for intracrystalline creep commonly observed in antigorite (12). In the absence of high-pressure data, quantifying the role of serpentinite at long and short time scales in subduction zones has remained beyond reach. We performed in situ measurements (13) of antigorite flow stress using the recently developed deformation-DIA (D-DIA) apparatus coupled with synchrotron x-ray analysis (14) under conditions of low constant strain rates ($\sim 10^{-4}$ to 10^{-6} s $^{-1}$) and pressure and temperature (P - T) of 1 and 4 GPa and 200° to 500°C, respectively; that is, over most of the antigorite stability field (4, 15). We obtained a stress-strain curve for 14 sets of experimental conditions (tables S1 and S2). Strain values $\epsilon(t)$ were measured on synchrotron x-ray radiographs, and differential stress σ was measured from elastic lattice strains on angle-dispersive x-ray diffraction patterns (13, 16). The stress value taken or extrapolated at 15% axial strain was used arbitrarily as a measure of the ultimate flow stress (table S3). Because sample observation shows features consistent with intracrystalline deformation (13), flow stress values were fitted to power-law equations (Table 1), in which the stress exponent depends on the dominant deformation mechanism (dislocation creep, diffusion, etc.), and to an exponential law appropriate for low-temperature creep processes [the Peierls mechanism (13)]. The best fit to the present data, at 1 and 4 GPa, was obtained with a single power-law equation that yielded an activation volume of 3.2 ± 0.7 cm 3 mol $^{-1}$, activation energy of 8.9 ± 5.4 kJ mol $^{-1}$, and a stress exponent of 3.8 ± 0.8 (Table 1), consistent with deformation by dislocation creep. The decrease of the stress exponent with increasing pressure when fitting data at each pressure independently (13) is consistent with the activation of intracrystalline deformation mechanisms at the expense of frictional grain boundary sliding at low confining pressure.

The ductile deformation of antigorite observed above 1 GPa complements observations from previous triaxial experiments, showing brittle behavior of serpentinite below 0.7 GPa and a transition toward a distributed semi-brittle deformation up to 1 GPa (5, 11). If controlled by antigorite, the transition from brittle to ductile creep at the slab interface with either the crust or the mantle wedge should depend mainly on depth, while the thermal structure of the subduction zone exerts only minor effects. In the case of high porosity (microcracks) with reduced effective confining pressure, the transition depth may depend indirectly on temperature through the amount of water released by mineral dehydration.

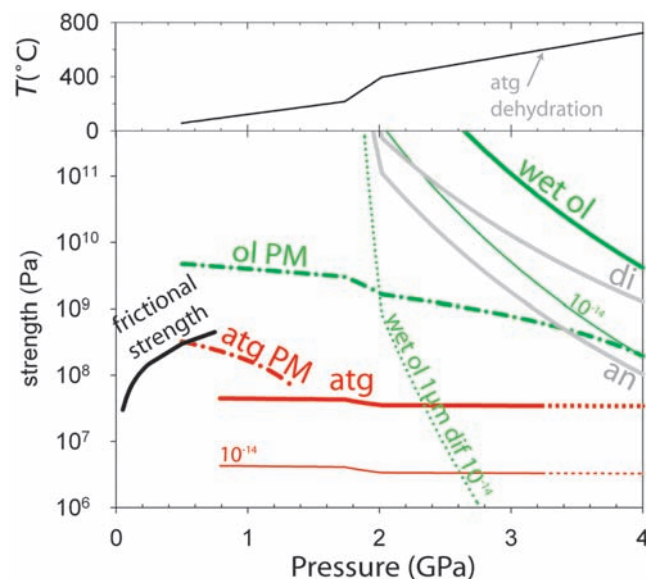
In order to depict further the potential role of antigorite rheology on wedge dynamics, we calculated a strength profile at a constant strain rate along a slab surface (Fig. 1), assuming a P - T profile in a moderately hot subduction zone and

considering two extreme cases. In the first model, we assumed a 300-m-thick serpentinite layer formed by hydration above the subducting slab and sheared by 10 cm year $^{-1}$, corresponding to a strain rate of 10^{-10} s $^{-1}$. Such conditions correspond to those of a subduction zone characterized by strong mechanical coupling or fast postseismic deformation due to sparse serpentinization. In the second case, a 10-km-thick serpentinite layer sheared by 1 mm year $^{-1}$ deforms at a strain rate of 10^{-14} s $^{-1}$. Such conditions hold for a subduction zone with a layer of extensively serpentinized mantle decoupled from a slowly downgoing slab. These two end-member models indicate that, regardless of strain rate and subduction-zone setting, antigorite is the only mineral among the major phases in the subducting lithosphere and mantle wedge that is capable of yielding by creep at geophysically relevant strain rates and temperatures below 600°C (Fig. 1).

Table 1. Preferred fits to power law $\dot{\epsilon} = A\sigma^n \exp[-(E_a + PV^*)/(RT)]$ and exponential law $\dot{\epsilon}_p = A_p \exp[-(E_p/RT)(1 - \frac{\sigma}{\tau})^2]$. Standard errors (1σ) are in parentheses at the right of each parameter. A and A_p are material constants, E_a and E_p are activation energies, V^* is activation volume, n is a stress exponent, and τ is Peierls stress.

Data used		Power law				
	$10^{-1} \ln(A)$	E_a (kJ)	V^* (cm 3)	n	R^2	
1 and 4 GPa	-8.6 (1.6)	8.9 (5.4)	3.2 (0.7)	3.8 (0.8)	0.89	
1 GPa	-12.6 (2.5)	17.6 (6.5)		5.8 (1.3)	0.90	
4 GPa	-7.9 (2.8)	16.6 (10.5)		3.4 (1.4)	0.81	
Data used		Exponential law				
	τ (GPa)	E_p (kJ)	$10^4 A_p$	R^2		
1 GPa	1.97 (0.36)	59.9 (18.4)	9.8 (2.5)	0.83		

Fig. 1. Strength of antigorite (atg) and other major silicates along a slab surface. Strengths are calculated from deformation laws at a strain rate of 10^{-10} s $^{-1}$ (thick curves) and 10^{-14} s $^{-1}$ (thin curves) along a slab surface P - T profile [profile number i50 from (28)] (upper graph). The low-temperature dislocation glide Peierls mechanism (PM) (29), is the most realistic deformation mechanism for olivine (ol) at these pressure, temperature, and strain-rate conditions. Because the Peierls mechanism cannot be extrapolated to low strain rates, strength can be calculated from the creep law only at 10^{-14} s $^{-1}$. At 10^{-10} s $^{-1}$, the transition from frictional behavior according to Byerlee's law (thick black line), and antigorite deforming plastically by the Peierls mechanism, occurs between 0.7 and 1 GPa. Antigorite strength remains at least one order of magnitude lower than that of other major mantle and crust minerals regardless of the deformation mechanism and the strain rate, except for very fine-grained (1 μ m) olivine deforming by diffusion creep (dif, dotted curve), the strength of which becomes inferior to that of antigorite before its dehydration at strain rates below $\sim 10^{-12}$ s $^{-1}$. Millimeter-sized olivine deforming by diffusion creep yields much higher strength and plots off the graph. The Peierls mechanism is from (29) and the wet olivine dislocation creep and diffusion creep from (30). di, wet diopside; an, anorthite, dislocation creep laws (31).



The exception is fine-grained olivine, which may become weaker than antigorite above 2.5 GPa (Fig. 1). Shear instabilities may, therefore, be reconsidered as a possible mechanism for intermediate-depth seismicity, which may either be related to antigorite dehydration producing very fine-grained olivine or occur within fine-grained partly serpentinized peridotites (17).

These deformation experiments provide an upper bound for serpentinite viscosity, because naturally occurring localizations would induce high strain rates and lower the effective viscosity. The values we calculated for effective serpentinite viscosity, $\sim 4 \cdot 10^{19}$ Pa*s for a strain rate of 10^{-13} s⁻¹ (13), are of the same orders of magnitude as those used in current numerical models (18). Serpentine viscosity as determined by us does not vary much with temperature, which precludes substantial shear heating in a low constant strain-rate system. Our flow law predicts that strain rate, hence viscosity as well, depends nonlinearly on stress. This would enhance positive feedbacks between strain and stress variations, as compared to models using linear stress dependence such as Newtonian rheology (18).

Seismologists define three zones downdip along the slab: seismic, transitional (locked during interseismic time), and aseismic. The factors controlling the downdip limit of the seismogenic and locked transitional zones will also govern the downdip propagation of megathrust ruptures,

such as the event of 26 December 2004 in Java (19). Because serpentinite has a low viscosity, with little pressure and temperature dependence above 1 GPa, the depth at which nonseismogenic creep is possible is governed exclusively by the extent of the serpentinite layer in the subduction zone. This is consistent with observations in Japan, where shallow depths (a maximum of 30 km) of seismogenic zones are associated with Poisson ratios higher than 0.29 (20), a strong indication of serpentinization, whereas deeper (50 to 70 km) downdip limits coincide with no indices of serpentinization (21). In Sumatra, where no evidence of serpentinization is found, the downdip limit occurs even deeper in the mantle (22).

Because of its low viscosity, serpentine can relax stress at rates comparable to those of postseismic and slow seismic deformations. Using a modified Maxwell body with a nonlinear viscous behavior, subject to a permanent deformation ϵ_0 producing an initial stress $\sigma_0 = \epsilon_0 E$, where E is the Young modulus (in pascals), the characteristic relaxation time τ_c required to relax half of the initial stress σ_0 is

$$\tau_c = \frac{2^{n-1} - 1}{AE(n-1)\sigma_0^{n-1}} \exp\left(\frac{E_a + PV^*}{RT}\right) \quad (1)$$

(23), where E_a and V^* are the activation energy and volume, respectively; A and n are material parameters; R is the gas constant; P is the

effective confining pressure; and T is the temperature. At temperatures of 200° to 500°C relevant to a slab surface, the relaxation times for antigorite are at least 10 orders of magnitude shorter than those for olivine (Fig. 2). For subduction-zone flow stress estimates up to ~ 100 MPa (18), antigorite relaxation times compare well with characteristic times of co- or postseismic surface deformations such as those measured by geodetic measurements for slow slip events, episodic tremor and slip, silent earthquakes, afterslips, and viscous relaxation (Fig. 2). Viscous relaxation of serpentinite therefore accounts for slow-slip events and for slow earthquakes occurring over periods of a few days to 1 year and which follow a scaling law different from that for regular earthquakes (24). These results also suggest that the importance of viscoelastic relaxation processes for triggering large earthquakes in subduction zones over interseismic periods of several years (25, 26) should be reassessed, taking into account the low viscosity of serpentinites measured here. Thus, the triggering of future earthquakes, such as the Tokai event expected in Japan, may depend on serpentinite viscous relaxation (7).

Together with a strong stress dependence, the low viscosity of antigorite at P - T conditions where other minerals have viscosities orders of magnitude higher confirms that serpentinite is an ideal candidate for strain localization within subduction zones. Moreover, antigorite-bearing serpentinites formed deeply in oceanic transform faults and passive margins may constitute decisive weak zones in the oceanic lithosphere, because their viscosity is lower than the critical value of 10^{20} Pa*s required to initiate subduction (27). The present data quantitatively relate viscous deformation of serpentinites to interseismic deformation and slow earthquakes. They should help improve numerical modeling of seismicity and convection in subduction zones.

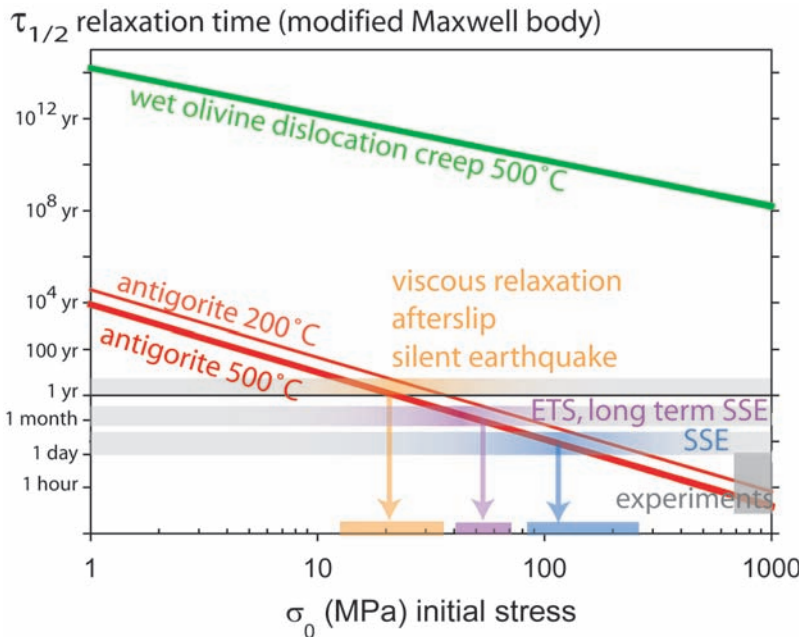


Fig. 2. Maxwell relaxation time for antigorite rheology and post- and slow seismic deformation time scales. $\tau_{1/2}$ is the time calculated (Eq. 1) to relax half of an initial stress σ_0 imposed at $t = 0$ (for instance, by the displacement field of an earthquake occurring close to a serpentinite body), using the antigorite power-law equation at 2 GPa (table S4) and $E = 89$ GPa (20). Stress above 20 MPa will be half-relaxed in less than 1 year by antigorite at 500°C (~ 40 MPa at 200°C), whereas stress relaxation is not possible in wet olivine deforming by dislocation creep (30) at these temperatures. Olivine diffusion creep (30), not reported here, leads to a constant characteristic relaxation time of $\sim 10^7$ years. Relaxation of high natural stress by antigorite flow is compatible with the time scales of postseismic deformation after large earthquakes (7, 8, 25, 26) and slowslip events or silent earthquakes (24). ETS, episodic tremor and slip; SSE, slow slip events.

References and Notes

1. G. A. Abers, *Phys. Earth Planet. Int.* **149**, 7 (2005).
2. H. Kawakatsu, S. Watada, *Science* **316**, 1468 (2007).
3. W. S. Fyfe, A. R. McBirney, *Am. J. Sci.* **275A**, 285 (1975).
4. P. Ulmer, V. Trommsdorff, *Science* **268**, 858 (1995).
5. C. B. Raleigh, M. S. Paterson, *J. Geophys. Res.* **70**, 3965 (1965).
6. S. M. Peacock, R. D. Hyndman, *Geophys. Res. Lett.* **26**, 2517 (1999).
7. P. A. Rydelek, I. S. Sacks, *Earth Planet. Sci. Lett.* **206**, 289 (2003).
8. C. Zweck, J. T. Freymueller, S. C. Cohen, *Phys. Earth Planet. Int.* **132**, 5 (2002).
9. S. A. F. Murrell, I. A. H. Ismail, *Tectonophysics* **31**, 207 (1976).
10. E. H. Rutter, K. H. Brodie, *J. Geophys. Res.* **93**, 4907 (1988).
11. J. Escartin, G. Hirth, B. W. Evans, *J. Geophys. Res.* **102**, 2897 (1997).
12. A.-L. Auzende et al., *Eur. J. Mineral.* **14**, 905 (2002).
13. Materials and methods are available as supporting material on Science Online.
14. Y. Wang, W. B. Durham, I. C. Getting, D. J. Weidner, *Rev. Sci. Instrum.* **74**, 3003 (2003).
15. N. Hilairet, I. Daniel, B. Reynard, *Geophys. Res. Lett.* **33**, L02302 (2006).
16. T. Uchida, N. Funamori, T. Yagi, *J. Appl. Phys.* **80**, 739 (1996).

17. J. M. Warren, G. Hirth, *Earth Planet. Sci. Lett.* **248**, 438 (2006).
18. T. V. Gerya, B. Stoeckert, A. Perchuk, *Tectonics* **21**, 1056 (2002).
19. C. Subarya *et al.*, *Nature* **440**, 46 (2006).
20. N. I. Christensen, *Int. Geol. Rev.* **46**, 795 (2004).
21. T. Seno, *Earth Planet. Sci. Lett.* **231**, 249 (2005).
22. M. Simoes, J. P. Avouac, R. Cattin, P. Henry, *J. Geophys. Res. Solid Earth* **109**, B10402 (2004).
23. D. L. Turcotte, G. Schubert, *Geodynamics* (Cambridge Univ. Press, ed. 2, 2002).
24. S. Ide, G. C. Beroza, D. R. Shelly, T. Uchide, *Nature* **447**, 76 (2007).
25. A. M. Freed, R. Burgmann, *Nature* **430**, 548 (2004).
26. H. Ueda, M. Ohtake, H. Sato, *J. Geophys. Res. Solid Earth* **108**, 2151 (2003).
27. K. Regenauer-Lieb, D. A. Yuen, J. Branlund, *Science* **294**, 578 (2001).
28. J. A. Conder, *Phys. Earth Planet. Int.* **149**, 155 (2005).
29. P. Rateron, Y. Wu, D. J. Weidner, J. Chen, *Phys. Earth Planet. Int.* **145**, 149 (2004).
30. S. Karato, D. C. Rubie, H. Yan, *J. Geophys. Res. Solid Earth* **98**, 9761 (1993).
31. A. Dimanov, G. Dresen, *J. Geophys. Res. Solid Earth* **110**, B07203 (2005).
32. We thank B. Van de Moortèle for the electron microscopy and J. Blichert-Toft, F. Albarède, J. Bass, and the two anonymous reviewers for their suggestions. This work was supported by the Institut National des Sciences de l'Univers (SEDIT program). The experiment was carried out at GeoSoilEnviroCARS (Sector 13) at the Advanced Photon Source (APS), Argonne National Laboratory. Use of the APS was supported by the U.S. Department of Energy (DOE), Office of Science, Office of Basic Energy Sciences, under contract no. DE-AC02-06CH11357. GeoSoilEnviroCARS is supported by NSF-Earth Sciences (grant EAR-0217473), DOE-Geosciences (grant DE-FG02-94ER14466), and the State of Illinois.

Supporting Online Material

www.sciencemag.org/cgi/content/full/318/5858/1910/DC1
Materials and Methods

Figs. S1 to S8
Tables S1 to S3

References

30 July 2007; accepted 7 November 2007

10.1126/science.1148494

A Comprehensive Phylogeny of Beetles Reveals the Evolutionary Origins of a Superradiation

Toby Hunt,^{1,2,*} Johannes Bergsten,^{1,2,*} Zuzana Levkanicova,³ Anna Papadopoulou,^{1,2} Oliver St. John,^{1,2} Ruth Wild,^{1,2} Peter M. Hammond,¹ Dirk Ahrens,⁴ Michael Balke,^{1,4} Michael S. Caterino,^{1,5} Jesús Gómez-Zurita,^{1,6} Ignacio Ribera,⁷ Timothy G. Barraclough,² Milada Bocakova,⁸ Ladislav Bocak,³ Alfried P. Vogler^{1,2,†}

Beetles represent almost one-fourth of all described species, and knowledge about their relationships and evolution adds to our understanding of biodiversity. We performed a comprehensive phylogenetic analysis of Coleoptera inferred from three genes and nearly 1900 species, representing more than 80% of the world's recognized beetle families. We defined basal relationships in the Polyphaga supergroup, which contains over 300,000 species, and established five families as the earliest branching lineages. By dating the phylogeny, we found that the success of beetles is explained neither by exceptional net diversification rates nor by a predominant role of herbivory and the Cretaceous rise of angiosperms. Instead, the pre-Cretaceous origin of more than 100 present-day lineages suggests that beetle species richness is due to high survival of lineages and sustained diversification in a variety of niches.

The extraordinary diversity of beetles has long fascinated evolutionary biologists (1). The strongly sclerotized front wings defining the order Coleoptera (the beetles), which provide protection while retaining the ability of powered flight with the membranous hindwings, may be an evolutionary novelty that promoted extensive diversification (2). Beetles appeared around 285 million years ago (Ma) (2, 3), followed by radiations of wood-boring (suborder

Archostemata), predacious (Adephaga), and fungivorous (Polyphaga) lineages (4) present in the fossil record from the middle Triassic on (2, 3). Their species richness is associated with extreme morphological, ecological, and behavioral diversity (4), and diversification of the most species-rich extant lineages may have been driven by co-radiations with angiosperms (5) and/or mammals (6) and/or geological and climatic change (7) occurring since the Cretaceous (145 to 65 Ma).

Studies of phylogenetic relationships within the Coleoptera resulted in a preliminary consensus on the classification, defining 4 suborders, 17 superfamilies, and 168 families (8–10). However, formal phylogenetic analyses of morphological characters (11, 12) and more recently molecular data (5, 13, 14) have been limited to subgroups at the family or superfamily level. Because of the sheer size of the group and the complexity of morphological character systems, these analyses have not been applied to the entire order.

We compiled a three gene data matrix providing a complete taxonomic representation for all suborders, series and superfamilies; >80% of recognized families; and >60% of subfamilies

(9, 10), which together contain >95% of described beetle species. Sequences for the small subunit ribosomal RNA (18 S rRNA) were obtained for 1880 species from de novo sequencing and existing databases. Mitochondrial 16S rRNA (*rnl*) and cytochrome oxidase subunit I (*coxI*) sequences were added for nearly half of these taxa (table S1) to create a data matrix of rapid, medium, and slowly evolving sequences. Phylogenetic analysis of the combined matrix was performed with a fragment-extension procedure for global sequence alignment followed by tree searches with fast parsimony algorithms (15). We tested for long-branch attraction, i.e., the spurious pairing of rapidly evolving lineages, by removing taxa terminal to long branches and assessing trees with a retention index (RI) measure of fit to the traditional classification (table S2) (15). The resulting parsimony tree largely agrees with the existing classification at the family and superfamily levels [on average, 95.7% of terminals assigned to a family were recovered as monophyla (table S2)], although our taxon sampling was not comprehensive in some families. Model-based Bayesian methods were applied to a 340-taxon representative subset at the subfamily level.

The trees (Figs. 1 and 2) were rooted with the neuropterid orders, the presumed sister to the Coleoptera (16), and recovered the major subdivisions of Adephaga [37,000 known species; posterior probability (*pp*) = 1.0] and Polyphaga (>300,000 species; *pp* = 1.0) as sisters to the Myxophaga (94 species) plus Archostemata (40 species) (8). The Adephaga was divided into two clades containing an aquatic (Hydradephaga; diving beetles and whirligig beetles; *pp* = 0.90) and a terrestrial (Geadephaga; ground beetles and tiger beetles; *pp* = 1.0) lineage, supporting a single terrestrial-to-aquatic transition in this suborder (13).

In the strongly supported suborder Polyphaga, five families occupied the basal nodes (Figs. 1 and 2) (*pp* = 1.0). These families include the Decliniidae; the Scirtidae, with aquatic larvae; the Derodontidae, an ecologically diverse family from global temperate zones; and the Eucinetidae and the Clambidae. These ancestral five families were previously considered basal Elateriformia (superfamily Scirtoidea), except for Derodontidae,

¹Department of Entomology, Natural History Museum, Cromwell Road, London SW7 5BD, UK. ²Department of Biology, Imperial College London, Silwood Park Campus, Ascot SL5 7PY, UK. ³Department of Zoology, Faculty of Science, Palacky University, tr. Svobody 26, 77146 Olomouc, Czech Republic. ⁴Zoologische Staatssammlung München, Münchhausenstrasse 21, 81247 München, Germany. ⁵Santa Barbara Museum of Natural History, 2559 Puesta del Sol Road, Santa Barbara, CA 93105–2998, USA. ⁶Fisiologia i Biodiversitat Molecular, IBMB-CSIC, Jordi Girona 18–26, 08034 Barcelona, Spain. ⁷Departamento de Biodiversidad y Biología Evolutiva, Museo Nacional de Ciencias Naturales, José Gutiérrez Abascal 2, 28006 Madrid, Spain. ⁸Department of Biology, Pedagogical Faculty, Palacky University, Purkrabska 2, 77140 Olomouc, Czech Republic.

*These authors contributed equally to the work.

†To whom correspondence should be addressed. E-mail: a.vogler@imperial.ac.uk

High-Pressure Creep of Serpentine, Interseismic Deformation, and Initiation of Subduction

Nadege Hilairat, Bruno Reynard, Yanbin Wang, Isabelle Daniel, Sebastien Merkel, Norimasa Nishiyama and Sylvain Petitgirard

Science **318** (5858), 1910-1913.

DOI: 10.1126/science.1148494

ARTICLE TOOLS

<http://science.sciencemag.org/content/318/5858/1910>

SUPPLEMENTARY MATERIALS

<http://science.sciencemag.org/content/suppl/2007/12/19/318.5858.1910.DC1>

RELATED CONTENT

<file:/contentpending:yes>

REFERENCES

This article cites 29 articles, 4 of which you can access for free
<http://science.sciencemag.org/content/318/5858/1910#BIBL>

PERMISSIONS

<http://www.sciencemag.org/help/reprints-and-permissions>

Use of this article is subject to the [Terms of Service](#)